

Magnetic trapping of atomic nitrogen (^{14}N) and cotrapping of NH ($X^3\Sigma^-$)

Matthew T. Hummon,^{1,2,*} Wesley C. Campbell,^{1,2} Hsin-I Lu,^{3,2} Edem Tsikata,^{1,2} Yihua Wang,^{1,2} and John M. Doyle^{1,2}

¹*Department of Physics, Harvard University, Cambridge, Massachusetts 02138, USA*

²*Harvard-MIT Center for Ultracold Atoms, Cambridge, Massachusetts 02138, USA*

³*School of Engineering and Applied Sciences, Harvard University, Cambridge, Massachusetts 02138, USA*

(Received 8 February 2008; published 12 November 2008)

We observe magnetic trapping of atomic nitrogen (^{14}N) and cotrapping of ground-state imidogen (^{14}NH , $X^3\Sigma^-$). Both are loaded directly from a room-temperature beam via buffer gas cooling. We trap approximately 1×10^{11} ^{14}N atoms at a peak density of $5 \times 10^{11} \text{ cm}^{-3}$ at 550 mK. The $12 \pm 4 \text{ s}$ $1/e$ lifetime of atomic nitrogen in the trap is consistent with a model for loss of atoms over the edge of the trap in the presence of helium buffer gas. Cotrapping of ^{14}N and ^{14}NH is accomplished, with 10^8 NH trapped molecules at a peak density of 10^8 cm^{-3} .

DOI: [10.1103/PhysRevA.78.050702](https://doi.org/10.1103/PhysRevA.78.050702)

PACS number(s): 34.50.-s, 37.10.Pq, 37.10.Gh

The rapidly growing diversity of cold and ultracold atomic and molecular systems has opened the way for new applications and for the study of physical systems with new interactions. Recent achievements have brought closer the realization of quantum information systems based on cold polar molecules [1,2] as well as different approaches to searches for physics beyond the standard model using cold molecules [3]. Recently, several interacting systems have been studied: a Bose-Einstein condensate with dipolar interactions [4], near-threshold inelastic collisions in cold polar molecules [5], inelastic collisions in ultracold atom-molecule systems [6,7], and laser cooling and magnetic trapping of non- S -state atoms [8,9]. However, the promise of these systems goes even further than these accomplishments in condensed-matter and atomic physics. One prominent example is in the realm of cold chemistry. Reactions in cold-gas-phase atom-molecule systems play a key role in dense interstellar clouds [10,11]. If cold cotrapped atoms and molecules could be created at sufficient density, the parameters characterizing these reactions could be studied in the laboratory. Such studies may also lead to the observation of novel chemical reaction pathways such as tunneling [12,13].

To bring these ideas in quantum information, new physics, and cold chemistry to fruition, collisions and interactions between cold and ultracold atoms and polar molecules must be understood. This requires high sample densities ($>10^{10} \text{ cm}^{-3}$). One promising route toward this is atom-molecule cotrapping. A significant step toward the observation of these collisions is the production of dense (10^{12} cm^{-3}), ultracold ground state polar molecules from bi-alkali-metal Feshbach molecules [14]. Photoassociation of ultracold bi-alkali-metal mixtures has produced magnetically and electrostatically trapped polar molecules at temperatures of hundreds of μK and densities of 10^4 – 10^5 cm^{-3} [15,16]. Alternatively, techniques for direct cooling and slowing of hot polar molecules, such as Stark deceleration [17] and buffer gas cooling [18], have produced trapped molecules at temperatures of tens to hundreds of mK and with densities of up to 10^8 cm^{-3} [17–20].

Cotrapping could provide low temperatures and higher density via sympathetic cooling. This is also a promising avenue toward the study of cold atom-molecule collisions. With this in mind, many are working to cotrap molecules with atoms, specifically laser-cooled alkali-metal atoms [21–25]. An important alternative to that approach is buffer-gas loading and magnetic cotrapping of non-alkali-metal atoms. To achieve cooling of molecules in a cotrapped system, the atoms can be cooled evaporatively, and these in turn can cool the molecules through collisions. If inelastic processes are limited, a rapid density increase would also occur. The selection of the most advantageous (lowest inelastic loss rate) atom-molecule pair has been investigated in detail [21–24]. First, the molecule should be Hund's case (b), where the electron spin is weakly coupled to the internuclear axis. NH, a molecule studied by many groups [26–28], is of this type. Second, the atomic partner should have low mass and low polarizability. Comparing the atom we have chosen, nitrogen (N), with a typical alkali-metal atom, rubidium (Rb), N has 1/6 the mass and 1/40 the polarizability [29,30]. Calculations of cold-collision properties for the ^{15}N - ^{15}N and ^{15}N - ^{14}N systems indicate favorable collision rates for atomic evaporative cooling [31]. Thus, this atom is set to be an excellent refrigerator, perhaps for a molecule like NH.

In this Rapid Communication we report the trapping of atomic nitrogen (^{14}N) and cotrapping of ^{14}N with ground-state imidogen radicals (^{14}NH , $X^3\Sigma^-$). The apparatus, shown in Fig. 1, is similar to that described in Ref. [26]. Briefly, a cylindrical copper buffer-gas cell is thermally anchored to a ^3He refrigerator and is filled with ^3He buffer gas to a density of $(3 \text{ to } 10) \times 10^{14} \text{ cm}^{-3}$ at a temperature of about 550 mK. The buffer gas cell is surrounded by a pair of superconducting coils that produce a spherical quadrupole trapping field with maximum trap depth of 3.9 T. Cell windows are located both axially and radially along the cell to allow optical access for laser-induced fluorescence spectroscopy of the trapped species. The atoms and molecules are loaded into the buffer gas cell via a molecular beam that enters the cell through a 1-cm aperture at the edge of the trapping region.

To produce the high-flux beam of atomic nitrogen we use an inductively coupled radio-frequency (rf) plasma source [32] operating in high-brightness mode [33]. The plasma

*matt@cua.harvard.edu

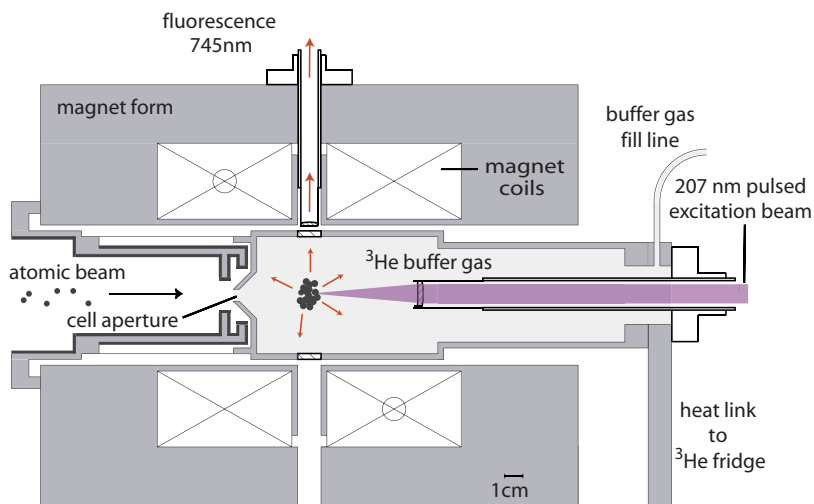


FIG. 1. (Color online) Diagram of trapping apparatus. The nitrogen atomic beam is produced by a rf plasma source located 23 cm to the left of the cell aperture. A lens is mounted inside the buffer gas cell 60 mm from the trap center to attain saturation of the two-photon transition for atomic nitrogen. The trapping magnet surrounds the buffer-gas cell and is described further in Ref. [26].

source generates a flux of atomic nitrogen of about 10^{16} atoms s^{-1} sr^{-1} [33]. The aperture of the plasma source is located about 23 cm from the entrance to the trapping cell. As the plasma source is run continuously during the experiment, a shutter, heat sunk at a temperature of 77 K, is located between the plasma source and the trapping cell. To load atoms or molecules into the cell, the shutter is pulsed opened for 20 ms and typically operates at a repetition rate of 4 Hz for continuous loading of the magnetic trap.

For detection of magnetically trapped ground-state atomic nitrogen, we use two-photon absorption laser-induced fluorescence (TALIF) [34], as the most accessible single-photon transition is at 120 nm [35]. We excite atomic nitrogen in the ground $(2p^3)^4S_{3/2}$ state with two photons at 207 nm to the excited $(3p)^4S_{3/2}$ state at $96\,750\text{ cm}^{-1}$. To generate the 207-nm light used for excitation we use third-harmonic generation of 620-nm light generated by a nanosecond-pulsed dye laser via nonlinear frequency conversions in KDP and BBO crystals. In order to generate the high intensities necessary to excite the two-photon transition, a 60-mm-focal-length lens is mounted in the buffer-gas cell and used to focus ≈ 1 mJ of 207-nm light to a $1/e^2$ waist diameter of $\approx 40\ \mu\text{m}$ at the trap center. Using a lens mounted at the midplane of the trapping magnet, we collect the atomic fluorescence at ≈ 745 nm from the decay of the excited $(3p)^4S_{3/2}$ state to the $(3s)^4P$ state and detect it using a photomultiplier tube (PMT). The pulse duration of the excitation light is about 10 ns, and the lifetime of the excited $(3p)^4S_{3/2}$ state is about 26 ns [36], which allows us to detect a temporally resolved fluorescence signal from the atomic nitrogen, shown in the inset of Fig. 2. Detection of NH is performed using laser-induced fluorescence (LIF) excited on the $|A^3\Pi_2, v'=0, N'=1\rangle \leftarrow |X^3\Sigma^-, v''=0, N''=0\rangle$ transition. The NH fluorescence is collected by the same lens that collects ^{14}N fluorescence and, using a dichroic mirror, is sent to a separate PMT for detection.

Figure 2 shows the TALIF spectrum of trapped ^{14}N taken during continuous loading of the magnetic trap. The spectrum fits well to a Lorentzian line shape with a full width at half maximum of 0.6 cm^{-1} . Measurements of the TALIF signal versus excitation laser pulse energy show a linear relationship, indicating that we achieve saturation of the TALIF

transition. The experimental TALIF linewidth is likely due to a combination of the laser linewidth (specified as 0.15 cm^{-1}) and saturation effects, as the Doppler width and Zeeman broadening of the two-photon transition are negligible. Precise estimation of the peak density of atomic nitrogen in the trap using the TALIF measurements is challenging, as accurate knowledge of fluorescence collection efficiency, effective TALIF excitation volume, and fluorescence yield per laser pulse is required. Furthermore, the pulsed dye laser generates multimode excitation light with a non-Gaussian spatial profile and a spectral profile that changes from shot to shot. Also, since a single 207-nm photon can photoionize the excited $(3p)^4S_{3/2}$ state of nitrogen, it is likely that a significant fraction (of order unity) of the excited nitrogen atoms undergo photoionization instead of fluorescence. In our data collection, we average the fluorescence over a large number of excitation pulses, typically about 100, so that the data yielded represent fluorescence taken over a range of saturations.

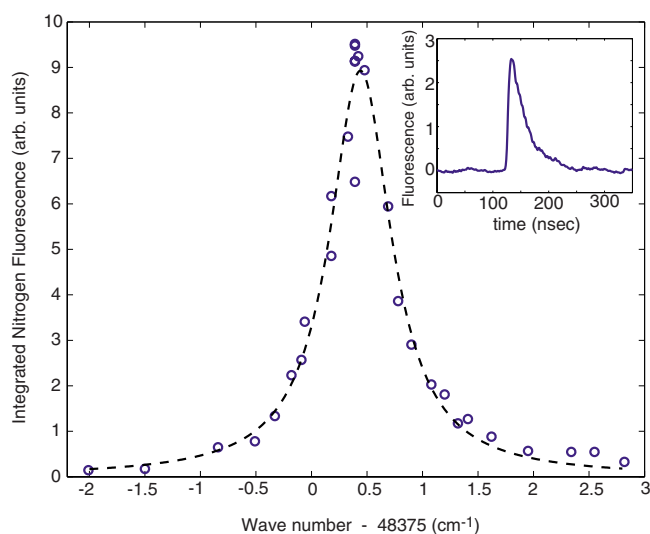


FIG. 2. (Color online) Integrated nitrogen fluorescence vs excitation wave number. The data (circles) are an average of 100 fluorescence acquisitions taken during continuous trap loading. The dashed line is a fit of the data to a Lorentzian. The inset shows time-resolved nitrogen fluorescence taken on resonance.

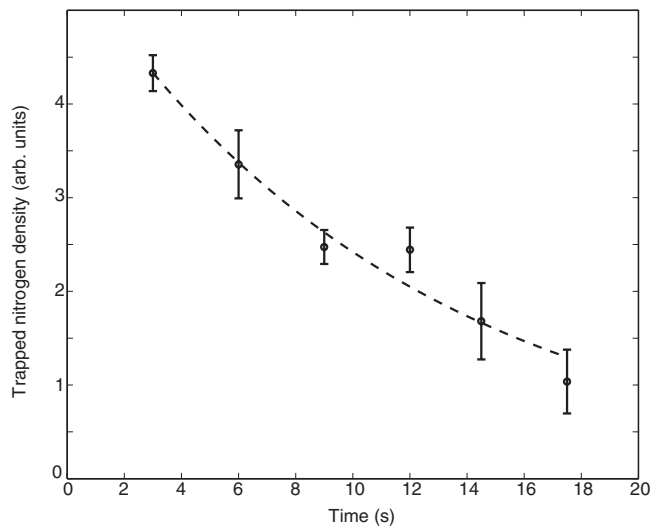


FIG. 3. Trapped nitrogen density vs time after trap loading. The error bars for each point represent the standard error for four sets of data. An exponential fit (dashed line) to the data yields a $1/e$ trap lifetime of 12 ± 4 s.

tion conditions. To estimate the effective excitation volume, we use a theoretical value of the two-photon cross section [37,38] and integrate the excitation probability over a Gaussian spatial profile for the 207-nm light of $1/e^2$ diameter of $40 \mu\text{m}$. Neglecting the effects of photoionization, the systematic uncertainties in the calculations of the fluorescence collection efficiency, and effective excitation volume yields an overall uncertainty of a factor of 3 in the peak density $n_{\text{N}} = 5 \times 10^{11} \text{ cm}^{-3}$ and total number $N_{\text{N}} = 1 \times 10^{11}$ of trapped nitrogen atoms. Including the effects of photoionization could increase the calculated number of trapped atoms by as much as a factor of 10 [39,40], so our determined N_{N} may be considered a lower bound.

Figure 3 shows the integrated TALIF signal of the ^{14}N in the magnetic trap versus time in the presence of ^3He buffer gas of density $(6 \pm 1) \times 10^{14} \text{ cm}^{-3}$ and temperature $530 \pm 20 \text{ mK}$. The $1/e$ trap lifetime of ^{14}N of 12 ± 4 s, where the quoted uncertainty is a 95% statistical error bound, is consistent with a model for loss of atoms over the edge of the trap in the presence of helium buffer gas [41]. If instead one assumes the observed loss is due entirely to inelastic ^{14}N - ^3He collisions, then this sets a limit on the ^{14}N - ^3He inelastic collision rate coefficient of $k_{\text{in}} < 2.2 \times 10^{-16} \text{ cm}^3 \text{ s}^{-1}$, corresponding to a limit of the ^{14}N - ^3He inelastic cross section of $\sigma_{\text{in}} < 3.3 \times 10^{-20} \text{ cm}^2$. Two possible inelastic collision channels for the ^{14}N - ^3He system are spin exchange between the electronic spin of ^{14}N and nuclear spin of ^3He and Zeeman relaxation induced by electronic interaction anisotropy [42]. Spin exchange rates for cold atoms with ^3He are typically small; the inelastic rate coefficient for the ^{52}Cr - ^3He system was measured to be $k_{\text{in}} = (2 \pm 1) \times 10^{-18} \text{ cm}^3 \text{ s}^{-1}$ [43]. Bismuth, though in the same group as nitrogen, has a large inelastic rate coefficient with ^3He of $k_{\text{in}} > 1.8 \times 10^{-14} \text{ cm}^3 \text{ s}^{-1}$ due to the electronic interaction anisotropy induced by spin-orbit coupling [44]. The small inelastic rate coefficient for ^{14}N - ^3He collisions is an indication that the electronic anisotropy for N-N collisions may also be small,

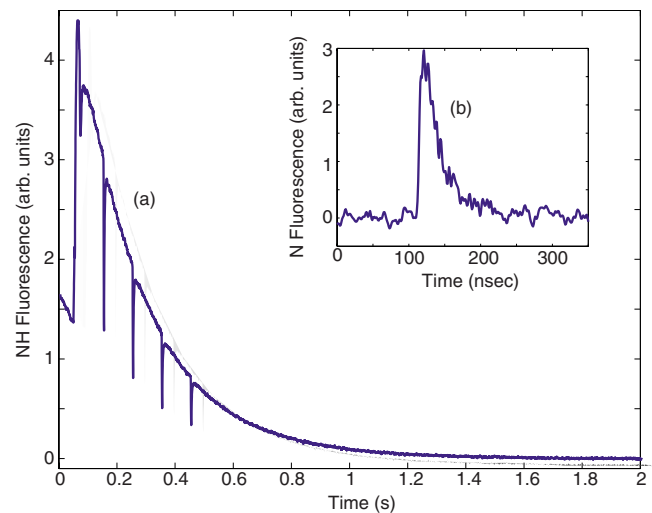


FIG. 4. (Color online) Cotrapping of N and NH, (a) shows trapped NH with a $1/e$ lifetime of 250 ms. (b) shows the average atomic nitrogen fluorescence signal taken during the first 0.5 s of trace (a). The downward spikes in trace (a) during the first 0.5 s correspond to the firing of the 207-nm excitation laser and the likely photodissociation of NH.

which opens the possibility for efficient evaporative cooling of atomic nitrogen.

To cotrap atomic nitrogen and NH radicals, we change the process gas for the rf plasma source. We find that both ammonia or a combination of molecular nitrogen and hydrogen work equally well for producing the trap species. Figure 4(a) shows the LIF signal of NH in the trap versus time. The NH has a $1/e$ trap lifetime of 250 ms, limited by inelastic Zeeman-state-changing collisions of NH with the helium buffer gas of density $(3 \pm 0.6) \times 10^{14} \text{ cm}^{-3}$ and temperature $550 \pm 20 \text{ mK}$ [26]. The LIF signal has been calibrated using laser absorption [20], and we trap about 10^8 NH molecules at peak densities of 10^8 cm^{-3} . The downward spikes in the NH profile in Fig. 4(a) correspond to the times at which the pulsed 207-nm laser fires for the atomic nitrogen detection. Figure 4(b) shows the average atomic nitrogen TALIF signal taken over the first 0.5 s of trapping, simultaneous with the trapping of NH shown in Fig. 4(a). The nitrogen fluorescence shown in Fig. 4(b) corresponds to about 4×10^{10} trapped ^{14}N atoms at a peak density of $1 \times 10^{11} \text{ cm}^{-3}$. In the future, we should be able to increase the number of atoms and molecules loaded into the trap by at least a factor of 4 simply by moving the plasma source closer to the trapping cell. The lifetimes of the cotrapped nitrogen and NH are long enough that thermal isolation via removal of the buffer gas should be possible [45] and is currently being pursued. Cotrapping of other atomic and molecular species can be performed using loading techniques such as laser ablation or loading from multiple molecular beams. Nitrogen cotrapped with a molecule is an excellent candidate for sympathetic cooling.

As mentioned in the beginning of this Rapid Communication, our work is important to understanding certain astrophysical phenomena. There is considerable interest in interstellar nitrogen, as recent astronomical observations have provided evidence that most interstellar nitrogen in the gas

phase is not, as previously thought, in molecular form, but rather in atomic form [11,46,47]. A network of cold chemical reactions [48] involving atomic nitrogen and neutral molecular radicals (OH, NO, CH, CN, and NH, in particular) [10,11,49] plays an important role in interstellar gas-phase chemistry models. Specifically, the existence of small barriers (~ 25 K) to these reactions is an important parameter and is beyond the sensitivity of current theoretical calculations [11]. Theoretical study of these reactions predicts rate constants on the order of $k \sim 10^{-11}$ cm³ s⁻¹ at temperatures of ~ 10 K [10,49], suggesting that the reactions may be observable using a cold, high-density sample of trapped atomic nitrogen, similar to what has been achieved here. Removing the buffer gas, as we have done previously in similar work, would open the door to this measurement [45].

In summary, we have observed magnetic trapping and cotrapping of atomic nitrogen and ground-state NH mol-

ecules. We trap approximately 1×10^{11} ¹⁴N atoms at a peak density of 5×10^{11} cm⁻³ and temperature of 550 mK with a $1/e$ trap lifetime of 12 ± 4 s. This lifetime sets a limit on the ¹⁴N-³He inelastic collision rate coefficient of $k_{in} < 2.2 \times 10^{-16}$ cm³ s⁻¹. Moreover, we cotrap about 4×10^{10} ¹⁴N atoms and 10^8 NH molecules at a temperature of 550 mK. If this system had the buffer gas removed [45], a wealth of research paths exist: evaporative cooling, possibly to quantum degeneracy, of a new atomic species, investigation of sympathetic cooling of polar molecules in a magnetic trap, and cold nitrogen chemistry.

We would like to thank Gale Petrich and Leslie Kolodziejewski for loan of the rf plasma source. This work was supported by the National Science Foundation under Grant No. 0457047, the U.S. Department of Energy under Contract No. DE-FG02-02ER15316, and the U.S. Army Research Office.

-
- [1] D. DeMille, Phys. Rev. Lett. **88**, 067901 (2002).
 [2] A. Andre *et al.*, Nat. Phys. **2**, 636 (2006).
 [3] M. G. Kozlov and L. N. Labzowsky, J. Phys. B **28**, 1933 (1995).
 [4] T. Lahaye *et al.*, Nature (London) **448**, 672 (2007).
 [5] J. J. Gilijamse *et al.*, Science **313**, 1617 (2006).
 [6] N. Zahzam, T. Vogt, M. Mudrich, D. Comparat, and P. Pillet, Phys. Rev. Lett. **96**, 023202 (2006).
 [7] P. Staunum, S. D. Kraft, J. Lange, R. Wester, and M. Weidemuller, Phys. Rev. Lett. **96**, 023201 (2006).
 [8] C. I. Hancox *et al.*, Nature (London) **431**, 281 (2004).
 [9] J. J. McClelland and J. L. Hanssen, Phys. Rev. Lett. **96**, 143005 (2006).
 [10] D. Edvardsson, C. F. Williams, and D. C. Clary, Chem. Phys. Lett. **431**, 261 (2006).
 [11] M. Akyilmaz *et al.*, Astron. Astrophys. (2007).
 [12] N. Balakrishnan and A. Dalgarno, Chem. Phys. Lett. **341**, 652 (2001).
 [13] R. V. Krems, Int. Rev. Phys. Chem. **24**, 99 (2005).
 [14] K.-K. Ni *et al.*, Science **322**, 231 (2008).
 [15] D. Wang *et al.*, Phys. Rev. Lett. **93**, 243005 (2004).
 [16] J. Kleinert, C. Haimberger, P. J. Zabawa, and N. P. Bigelow, Phys. Rev. Lett. **99**, 143002 (2007).
 [17] S. van de Meerakker, N. Vanhaecke, and G. Meijer, Annu. Rev. Phys. Chem. **57**, 159 (2006).
 [18] J. D. Weinstein *et al.*, Nature (London) **395**, 148 (1998).
 [19] B. C. Sawyer *et al.*, Phys. Rev. Lett. **98**, 253002 (2007).
 [20] W. C. Campbell, G. C. Groenenboom, Hsin-I Lu, E. Tsikata, and J. M. Doyle, Phys. Rev. Lett. **100**, 083003 (2008).
 [21] P. Soldan and J. M. Hutson, Phys. Rev. Lett. **92**, 163202 (2004).
 [22] M. Lara, J. L. Bohn, D. E. Potter, P. Soldan, and J. M. Hutson, Phys. Rev. A **75**, 012704 (2007).
 [23] M. Lara, J. L. Bohn, D. E. Potter, P. Soldan, and J. M. Hutson, Phys. Rev. Lett. **97**, 183201 (2006).
 [24] M. Tacconi, E. Bodo, and F. A. Gianturco, Theor. Chem. Acc. **117**, 649 (2007).
 [25] S. Schlunk *et al.*, Phys. Rev. Lett. **98**, 223002 (2007).
 [26] W. C. Campbell, E. Tsikata, Hsin-I Lu, L. D. van Buuren, and J. M. Doyle, Phys. Rev. Lett. **98**, 213001 (2007).
 [27] S. Hoekstra *et al.*, Phys. Rev. A **76**, 063408 (2007).
 [28] H. Lewandowski, L. P. Parazzoli, D. Lobser, and C. Romero (unpublished).
 [29] I. S. Lim *et al.*, Phys. Rev. A **60**, 2822 (1999).
 [30] J. Stiehler and J. Hinze, J. Phys. B **28**, 4055 (1995).
 [31] B. Zygelman (private communication).
 [32] Model CARS-25, Oxford Applied Research.
 [33] M. Moldovan *et al.*, J. Electron. Mater. **27**, 756 (1998).
 [34] S. F. Adams and T. A. Miller, Chem. Phys. Lett. **295**, 305 (1998).
 [35] Y. Ralchenko *et al.*, NIST atomic spectra database (version 3.1.3) [online], URL <http://physics.nist.gov/asd3>.
 [36] G. J. Bengtsson, J. Larsson, S. Svanberg, and D. D. Wang, Phys. Rev. A **45**, 2712 (1992).
 [37] K. Omidvar, Phys. Rev. A **22**, 1576 (1980).
 [38] K. Omidvar, Phys. Rev. A **30**, 2805 (1984).
 [39] D. J. Bamford, L. E. Jusinski, and W. K. Bischel, Phys. Rev. A **34**, 185 (1986).
 [40] K. L. Bell and A. E. Kingston, Adv. At., Mol., Opt. Phys. **32**, 1 (1994).
 [41] R. deCarvalho *et al.*, Eur. Phys. J. D **7**, 289 (1999).
 [42] R. Krems, G. Groenenboom, and A. Dalgarno, J. Phys. Chem. A **108**, 8941 (2004).
 [43] J. D. Weinstein, R. deCarvalho, C. I. Hancox, and J. M. Doyle, Phys. Rev. A **65**, 021604(R) (2002).
 [44] S. E. Maxwell *et al.*, Phys. Rev. A **78**, 042706 (2008).
 [45] J. Harris *et al.*, Europhys. Lett. **67**, 198 (2004).
 [46] S. Maret, E. A. Bergin, and C. J. Lada, Nature (London) **442**, 425 (2006).
 [47] D. C. Knauth, B.-G. Anderson, S. R. McCandliss, and H. W. Moos, Nature (London) **429**, 636 (2004).
 [48] A. Sternberg and A. Dalgarno, Astrophys. J., Suppl. Ser. **99**, 565 (1995).
 [49] T. J. Frankcombe and G. Nyman, J. Phys. Chem. A **111**, 13163 (2007).